Supplementary Figure S1

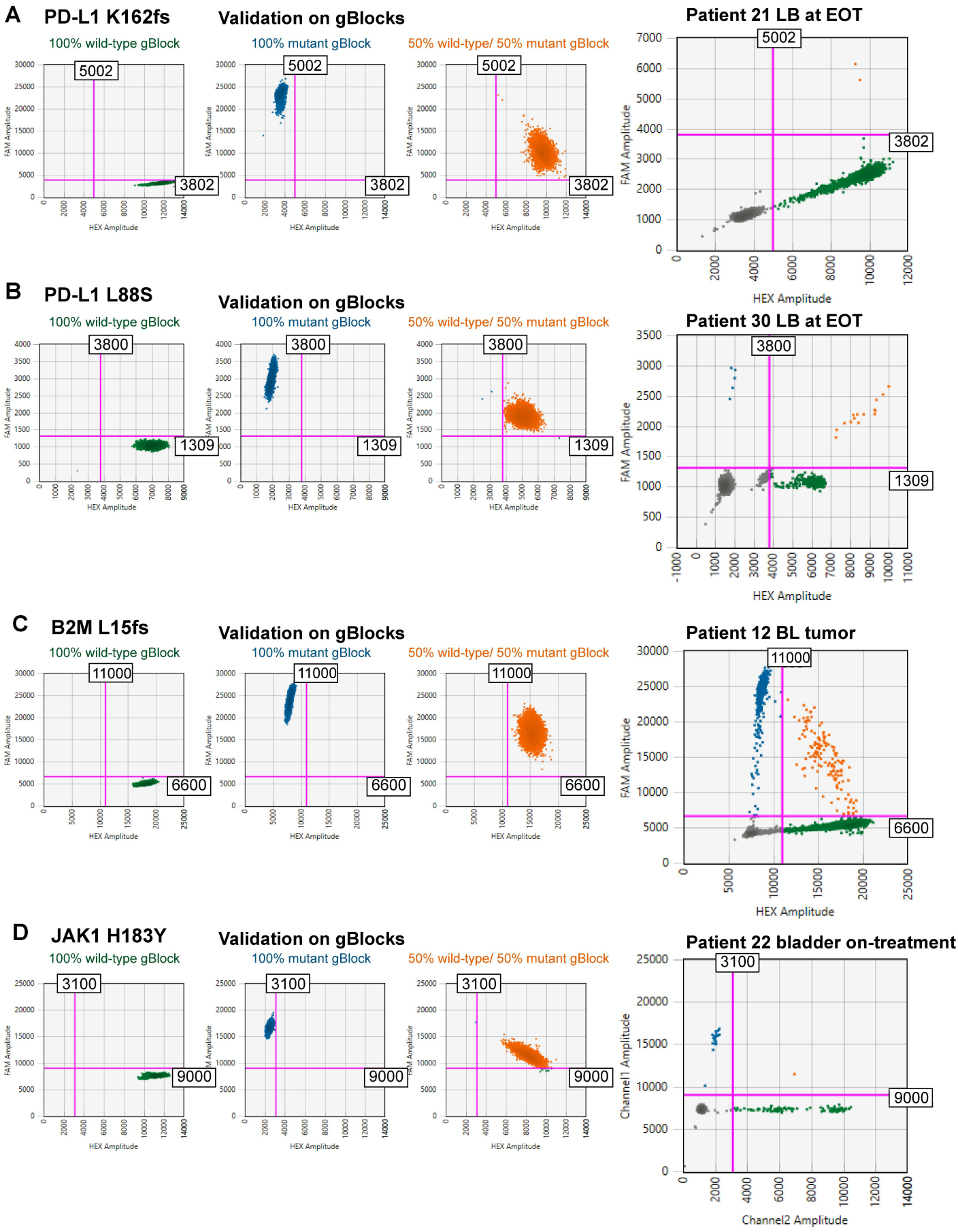

Supplementary Figure S2

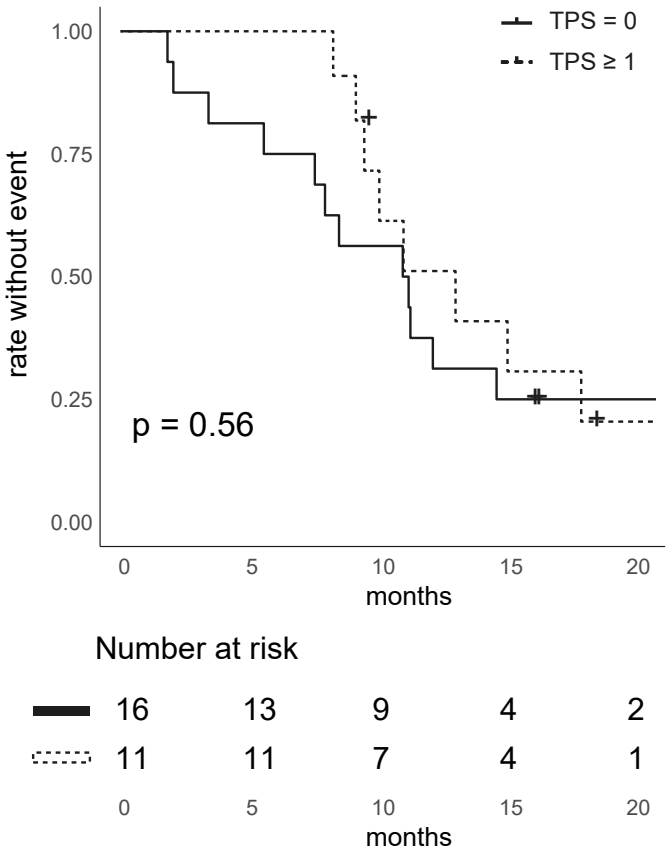

Supplementary Figure S3

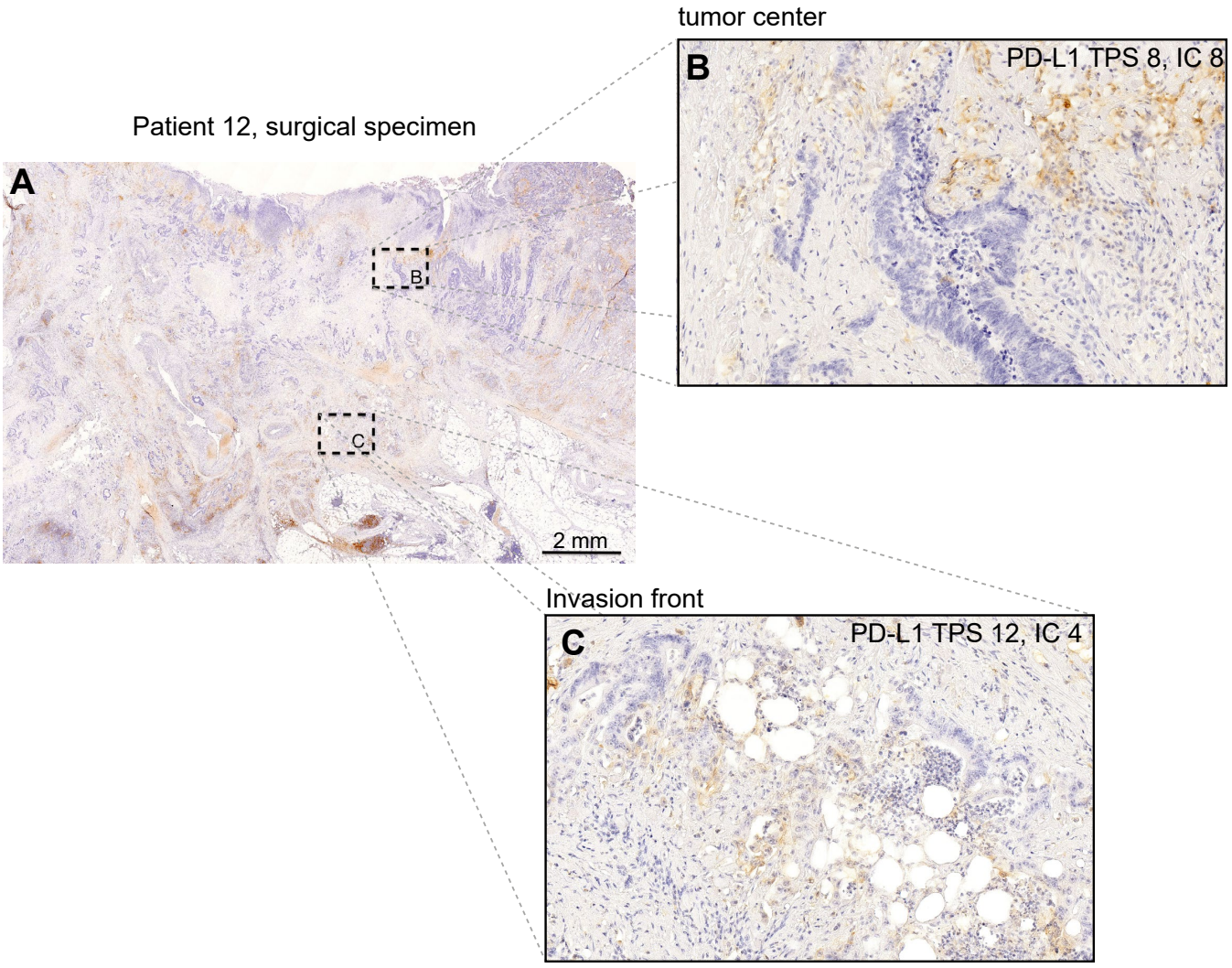

Supplementary Figure S4

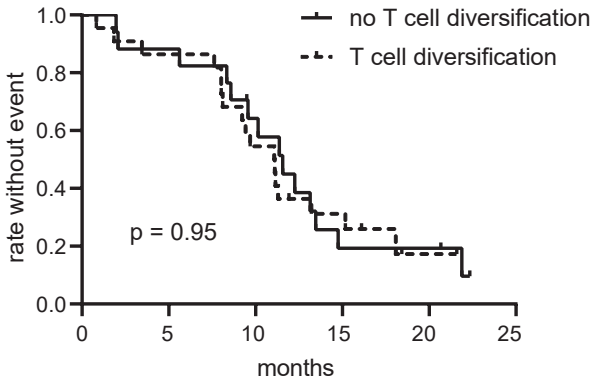

Supplementary Figure S5

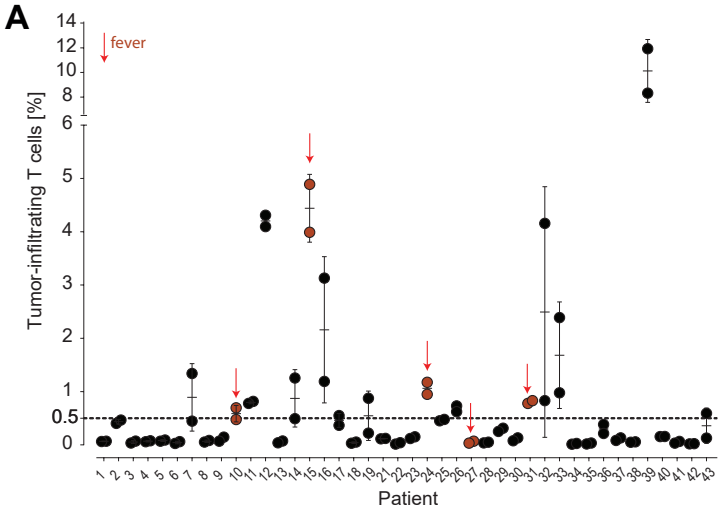

Supplementary Figure S6

A

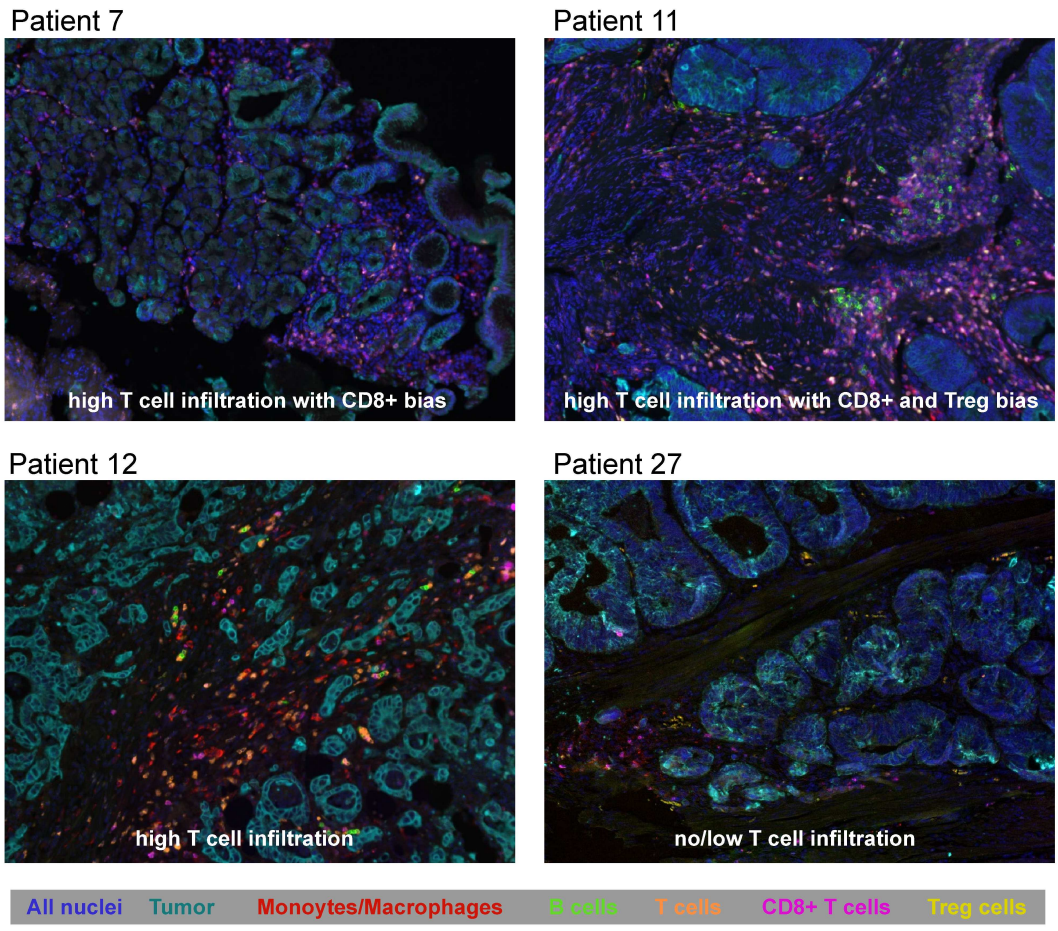

B

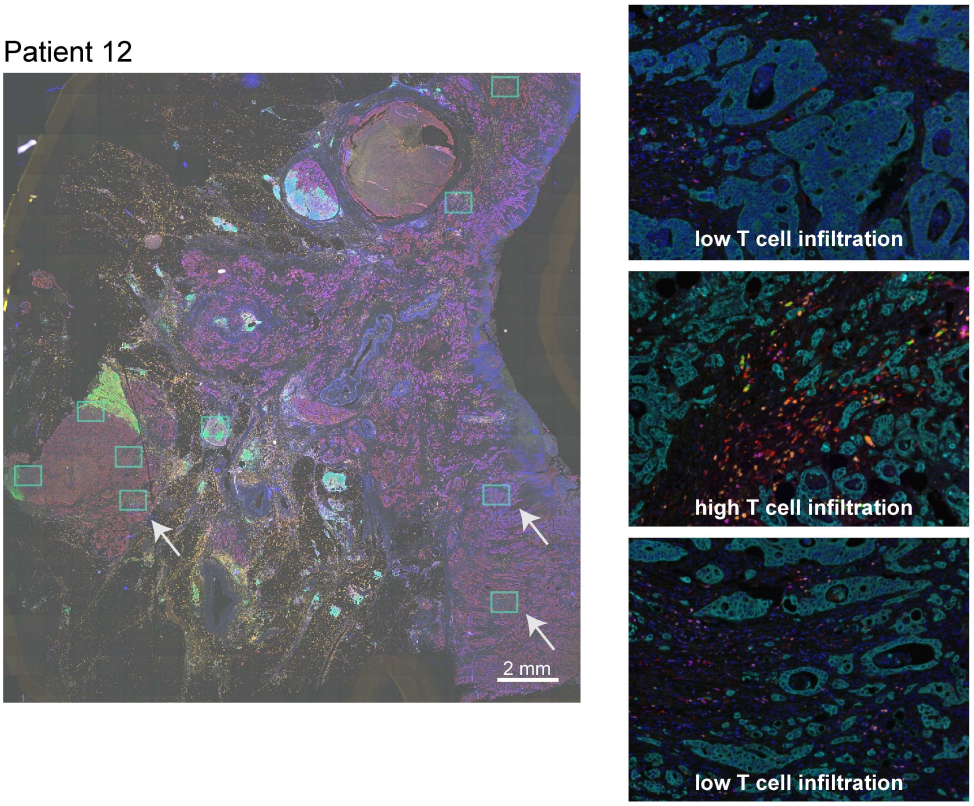

Supplementary Figure S7

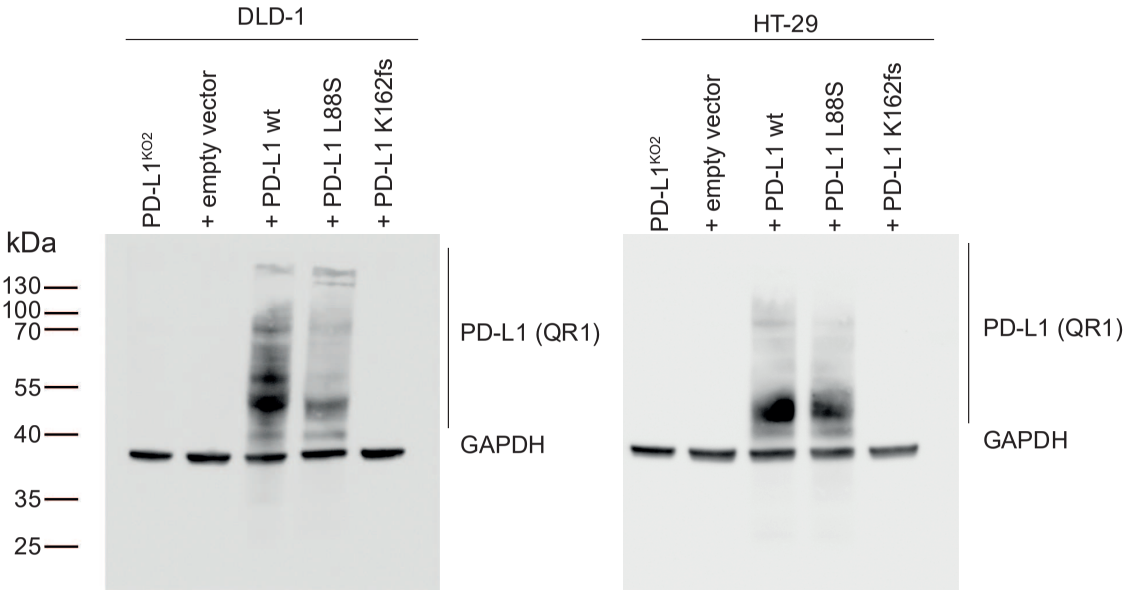

Stein A, *et al. J Immunother Cancer* 2021; 9:e002844. doi: 10.1136/jitc-2021-002844

Supplementary Figure S8

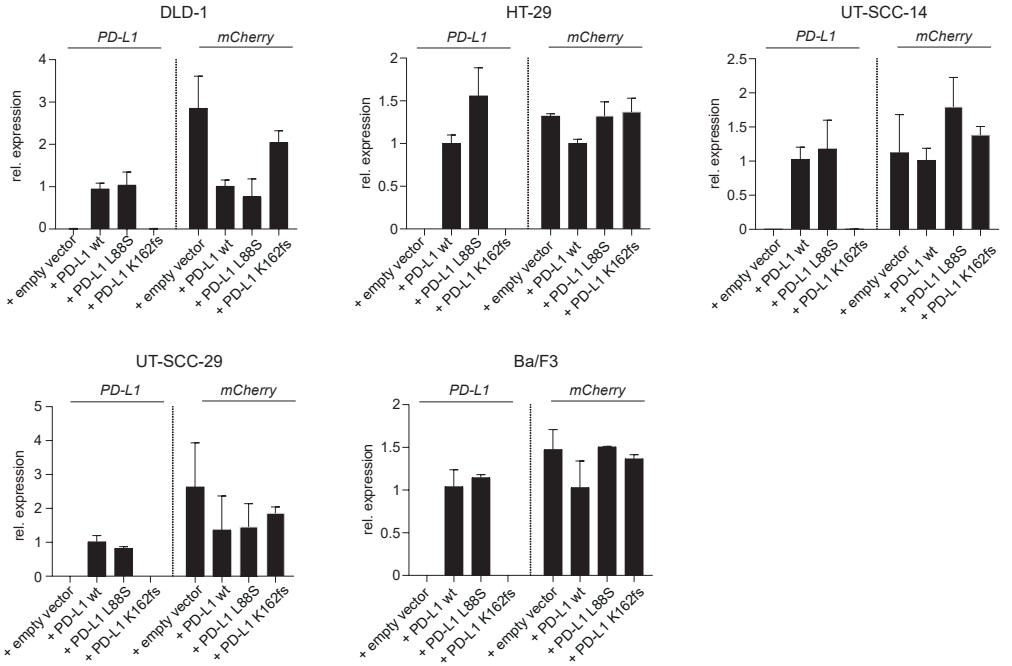

Supplementary Figure S9

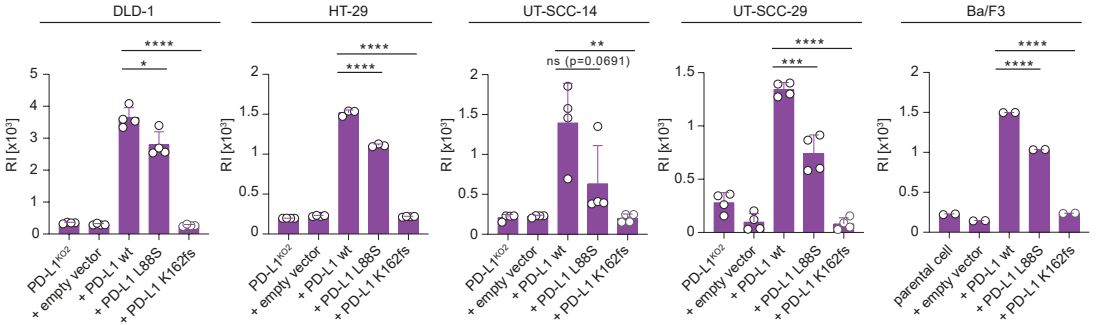

Supplementary Figure S10

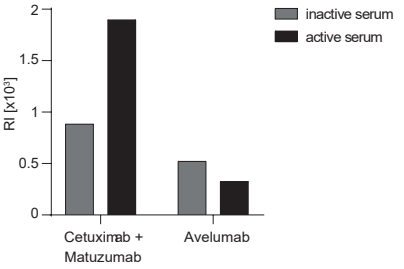

Supplementary Figure S11

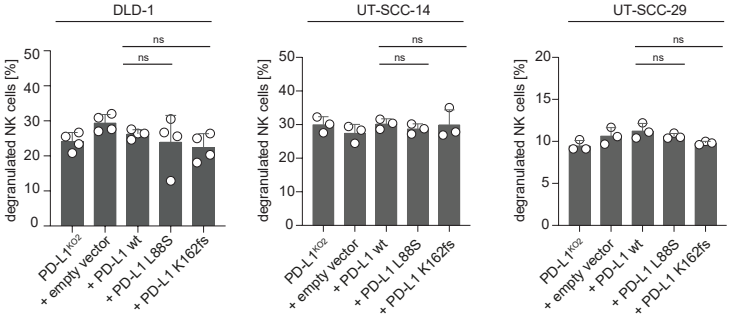

Supplementary Figure S12

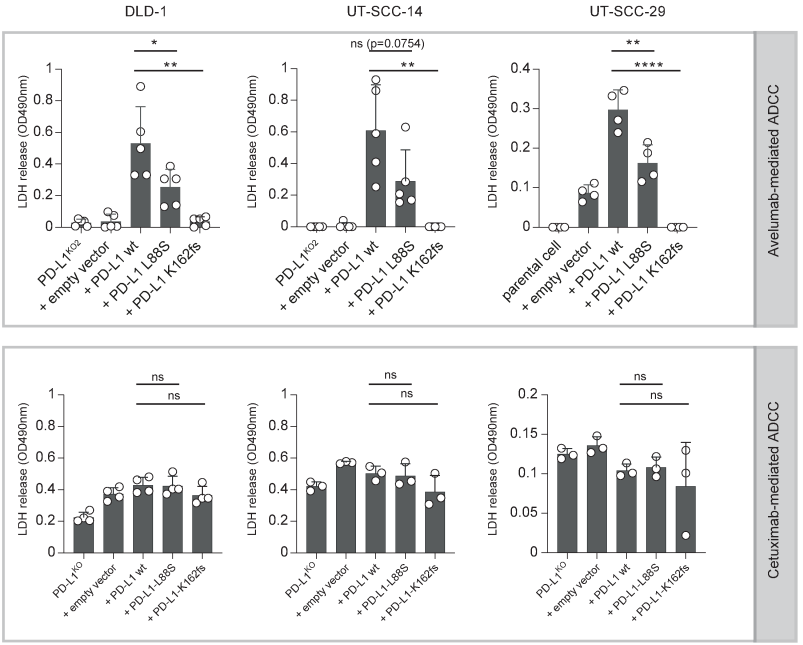

Supplementary Figure S13

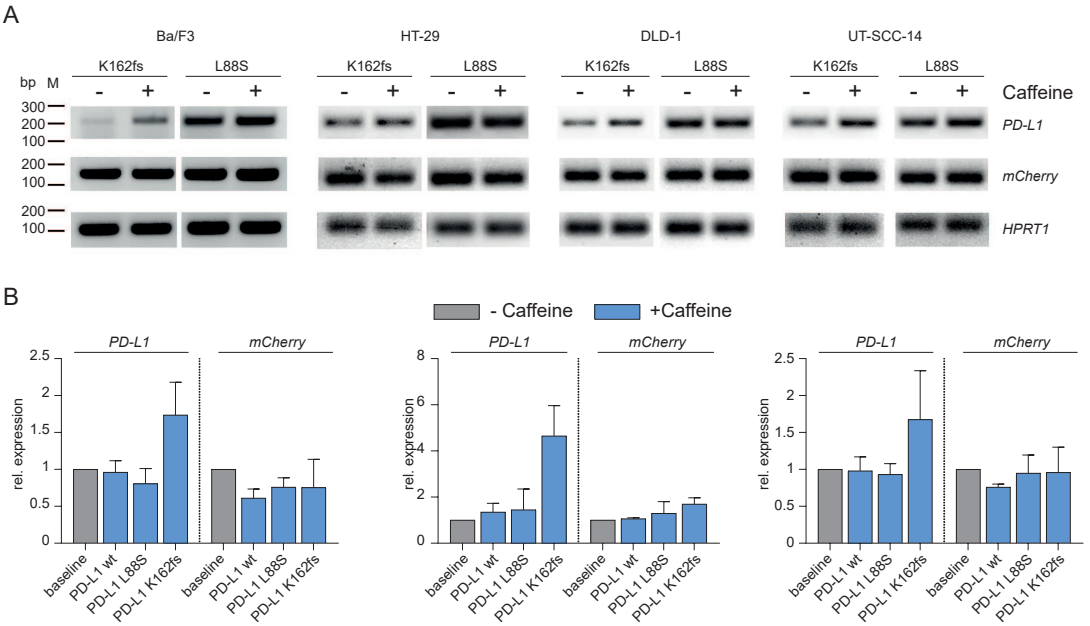

Supplementary Figure Legends

Fig. S1. Two-Dimensional plots for each ddPCR assay. (A) PD-L1 K162fs, (B) PD-L1 L88S, (C) B2M L15fs and (D) JAK1 H183Y. X-axis: HEX amplitude, Y-axis: FAM amplitude. Pink lines with adjacent number indicate thresholds for discrimination of positive/negative droplets. Left: Each assay was validated on gBlocks with the wild type or mutant sequence. Right: representative 2D plot for patient with respective variant.
BL, baseline; EOT, End of treatment; LB, liquid biopsy

Fig. S2. Tumor proportional score (TPS) and association with PFS. Kaplan Meier plot of progression-free survival stratified by TPS = 0 or TPS ≥ 1. Statistical-test: Log-rank test.

Fig. S3. Differences of PD-L1 positivity in tumor center vs. invasion front. A, Overview with marked areas of **B**, tumor center (B) and **C**, invasion front (C). *IC, immune cell score; TPS, tumor proportional score*

Fig. S4. Peripheral blood T cell diversification and association with PFS. Kaplan Meier plot of progression-free survival according to changes in peripheral blood T cell Shannon diversity between baseline and week 4 of AVETUX regimen. Statistical-test: Log-rank test.

Fig. S5. Tumor-infiltrating lymphocytes (TiL) quantification and association with PFS. A, Levels of TiLs across cohort. Patients with fever after avelumab application are marked with red arrows. Measurements performed in duplicates. Error bars indicate mean ±SD. **B,** Kaplan Meier plot of progression-free survival according to Tumor-infiltrating T cells. Statistical-test: Log-rank test.

Fig. S6. Assessment of immune cell infiltration by multispectral imaging. A, Representative stainings of four patients with heterogenous T cell infiltration levels ranging

from none/low infiltration to high/biased infiltration. B, Different areas of one tumor indicating intratumour heterogeneity of T cell infiltration.

Fig. S7. Immunodetection of PD-L1 variants using the QR1 antibody clone. Detection of PD-L1 protein levels using the QR1 antibody (Supplementary Table S3) after PAGE separation of whole cell extracts from PD-L1-KO DLD-1 and HT-29 cells ectopically re-expressing wt PD-L1 and the L88S and K162fs variants.

Fig. S8. qRT-PCR analysis of *PD-L1* transcript abundancy in cell lines ectopically expressing *PD-L1* variants. Cells transduced with indicated PD-L1 variants were subjected to qRT-PCR analysis to quantify *PD-L1* and *mCherry* transcript levels. The Ct values were normalized to *HPRT1* (*Hypoxanthine-guanine phosphorribosyltransferase*) and relative expression changes were calculated according to the ΔΔCt method.

Fig. S9. Flow cytometric detection of PD-L1 surface expression on cell lines. Flow cytometric detection of PD-L1 surface expression (n=2 for Ba/F3; n=3 for HT-29, n=4 for DLD-1, UT-SCC-14 and UT-SCC-29) displayed as the mean relative fluorescence intensity (RI) after staining with a FITC-labeled anti-PD-L1 antibody. Statistics: two-tailed unpaired t test. Asterisks indicate p-value range (*p<0.05; **p<0.01; ***p<0.001; ***p<0.0001; ns>0.05).

Fig. S10. Complement-dependent cytotoxicity in cell expressing PD-L1 wild-type. UT-SCC-14 cells were treated with avelumab and complement followed by PI staining. The combination of cetuximab and matuzumab was used as positive control.

Fig. S11. Cetuximab-mediated ADCC in DLD-1, UT-SCC14 and UT-SCC-29 cells. NK cell degranulation induced by co-culturing primary NK cells and DLD-1 (n=4), HT-29 (n=3) and UT-SCC-29 (n=3) cell lines expressing indicated *PD-L1* variants in the presence of

cetuximab. Percent degranulated NK cells normalized to spontaneous NK degranulation is shown for all co-cultures. Statistics: two-tailed unpaired t test. ns indicates p-values >0.05).

Fig. S12. Quantitation of antibody-dependent cytotoxicity in UT-SCC-29, UT-SCC-14 and DLD-1 cells expressing *PD-L1* variants. Colorimetric quantitation of lactate dehydrogenase (LDH) release from cell lines (n=3-5) expressing indicated *PD-L1* variants after co-culturing them with primary NK cells in the presence of avelumab. Detected LDH levels were normalized to spontaneous LDH release. Statistics: two-tailed unpaired t test. Asterisks indicate p-value range (*p<0.05; **p<0.01; ***p<0.001; ***p<0.0001; ns>0.05).

Fig. 13. PD-L1 K162fs is degraded via nonsense-mediated mRNA decay (NMD). Inhibition of NMD in PD-L1 wt, L88S and PD-L1 K162fs transduced Ba/F3, HT-29, DLD-1 and UT-SCC-14 cells using 20 mM caffeine for 4 h leads to a selective enrichment of PD-L1-K162fs transcript as detected by semiquantitative RT-PCR (A) and qRT-PCR (B). For qRT-PCR, Ct values were normalized to *HPRT1* (*Hypoxanthine-guanine phosphorribosyltransferase*) and relative expression changes were calculated according to the ΔΔCt method. mCherry: lentiviral transduction marker

Supplementary Table S1. Applied Antibodies.

Target	Epitope	Host	Isotype	Clone	Label	Working dilution	Supplier	Cat. No.	Used for
PD-L1	19-239	goat	polyclonal IgG		none	1:1000	R&D Systems	AF156	WB
PD-L1	C-term	rabbit	monoclonal IgG	E1L3N	non	1:1999	Cell Signaling	#13684	WB
PD-L1	full length	mouse	monoclonal IgG1	MIH2	FITC	1:300	Thermo Fisher	MA5-16841	FC
CD56		mouse	IgG1	N901	PE	1:20	Beckman Coulter	A07788	FC
CD107a		mouse	IgG1, kappa	H4A3	PE/Cy7	1:100	BioLegend	328618	FC
CD3		mouse	IgG1	UCHT1	FITC	1:20	Beckman Coulter	A07746	FC
CD3		mouse	monoclonal IgG2a, kappa	OKT3	none	100 ng/ml	BioLegend	317326	TA
CD28		mouse	monoclonal IgG1, kappa	CD28.2	none	100 ng/ml	BioLegend	302902	TA
p65	1-286	mouse	monoclonal IgG1		none	1:200	Santa Cruz	sc-8008	WB
PHB1	full length	mouse	monoclonal IgG2a, kappa		none	1 µg/ml	Abnova	H00005245-M01	WB
PHB2	220-299	mouse	monoclonal IgG1		none	1:200	Santa Cruz	sc-133094	WB
GAPDH	full length	mouse	monoclonal IgG1	6C5	none	1:200	Santa Cruz	sc-32233	WB
mouse-IgG (IgG1, IgG2a, IgG2b, IgG3)		goat			HRP	1:1000	R&D	HAF007	WB
rabbit-IgG		goat			HRP	1:10000	Sigma-Aldrich	A6154	WB
goat-IgG (IgG1, IgG2a, IgG2b, IgG3, IgG4)		mouse			HRP	1:5000	Santa Cruz	sc-2354	WB
mouse-IgG (IgG1, IgG2a, IgG2b, IgG3, IgM, IgA)		goat			IRDye 800CW	1:1000	Li-Cor	926-32210	WB
rabbit-IgG		goat			IRDye 680RD	1:1000	Li-Cor	926-68071	WB
human-IgG		rabbit			FITC	1:1000	Sigma-Aldrich	F4512	FC
PanCK		mouse		AE1/AE 3+5D3	none	1:50	Zytomed	MSG098	IHC
CD3	156-168	rabbit	IgG	SP7	none	1:50	Labvision (Thermo Fisher)	RM-9107	IHC
CD16		mouse	IgG2a	2H7	none	1:80	Leica	NCL-L-CD16	IHC
CD56		rabbit	IgG1	MRQ-42	none	1:250	Cell marque	156R-96	IHC
PD-L1		rabbit	IgG	QR1	none	1:100/1:1000	Quartett	1-PR292-02	IHC/WB
PD-L1		rabbit	IgG	CAL10	none	1:200	Zytomed	RBG063	IHC
CD3		rabbit	IgG	SP7	None	1 :100	Thermo Fisher	MA5-14524	MI
CD8		rabbit		SP16	None	1:100	Abcam	ab101500	MI
CD20		mouse		L26	None	1:400	Dako	M0755	MI
CD163		mouse		MRQ-26	None	1:50	Cell Marque	MRQ-26	MI
Foxp3		mouse		236A/E7	None	1:200	Abcam	ab20034	MI
panCK		mouse		AE1/AE 3	none	1:100	Dako	M3515	MI

WB, western blot; FC, flow cytometry; TA, T cell activation; IHC, immunohistochemistry; MI, multispectral imaging

Supplementary Table S2. Sequenced genes and gene regions.

Gene	Target Region
AKT1	codons 10-30
APC	codons 789 - 1589
B2M	entire coding region
BRAF	codons 582-605
CTNNB1	codons 30-46
EGFR	exon 12,13,18,19,20,21
ERBB3	codons 85-105
FCGR3A	codon 158
FCGR2A	codon 131
HRAS	codons 10-15
JAK1	entire coding region
JAK2	entire coding region
KRAS	codons 10-15, 51-63, 98-150
NRAS	codons 10-15, 51-63
PIK3CA	codons 64-94, 316-346, 418-434, 527-560, 1002-1054
PD-L1	entire coding region
PTEN	codons 71-124,130,173,267,268,320
SMAD4	entire coding region
TP53	entire coding region

Supplementary Table S3. Overview of all variants found by gene panels sequencing in all tissues and timepoints.

Table is provided as excel sheet.

Supplementary Table S4. ddPCR primer and probe sequences.

Assay			**Sequence 5´to 3´**	**5´Reporter dye**
PD-L1 L88S	forward	primer	CTGAAGGTTCAGCATAGTAGC	
	reverse	primer	TGCATCCTGCAATTTCACAT	
	wild-type	probe	CT+ACC+C+C+AAGGC	HEX
	mutant	probe	CT+A+CC+C+A+AG+GC	FAM
PD-L1 K162fs	forward	primer	ACCTCTGAACATGAACTGACAT	
	reverse	primer	CTCCTCTCTCTTGGAATTGGT	
	wild-type	probe	CTG+T+T+GA+AG+G+AC	HEX
	mutant	probe	CTG+T+C+GA+AG+GAC	FAM
JAK1 H183Y	forward	primer	TCTTCTTCATCATGGCATAGTGT	
	reverse	primer	GGTGAAATGCCTGGCTC	
	wild-type	probe	TCA+T+G+TC+CA+TCCT	HEX
	mutant	probe	TCA+T+A+TC+CAT+C+CT	FAM
B2M L15fs	forward	primer	GGCATTCCTGAAGCTGAC	
	reverse	primer	GAGAGACTCACGCTGGATA	
	wild-type	probe	CTA+CT+CTC+T+C+TTT+CT	HEX
	mutant	probe	CTA+CT+CTC+T+T+TCT+GG	FAM

Base after " + " is a locked nucleic acid base.

Supplementary Table S5. TPS and IC score with two different PD-L1 Antibody clones.

Pat ID	TPS(%) QR1	IC(%) QR1	TPS(%) CAL10	IC (%) CAL10	origin tumor sample	material type
1	0	30				surgical specimen
2	0	40				surgical specimen
3	0	50				surgical specimen
4	0	2				biopsy
5	0	15				surgical specimen
6	1	25				surgical specimen
7	n.e.	n.e.				biopsy
8	0	7	0	5	liver metastasis	surgical specimen
9	25	30				biopsy
10	n.e.	n.e.				surgical specimen
11	0	20	0	15		biopsy
12	4	40	4	35		surgical specimen
13	2	20				biopsy
14	n.e.	n.e.				surgical specimen
15	1	10				surgical specimen
16	1	20				surgical specimen
17	0	3	0	0		surgical specimen
18	n.e.	n.e.				surgical specimen
19	n.e.	n.e.				surgical specimen
20	1	6				biopsy
21	3	20				biopsy
22	10	0	8	0	bladder metastasis	surgical specimen
23	n.e.	n.e.				surgical specimen
24	5	10	1	6		biopsy
25	0	1	0	5		surgical specimen
26	0	0				biopsy
27	0	1	0	0		surgical specimen
28	2	5	0	1	lymph node metastasis	surgical specimen
29	0	30	0	15		biopsy
30	0	10	0	5	lymph node metastasis	surgical specimen
31	n.e.	n.e.				biopsy
32	0	3	0	3	lung metastasis	surgical specimen
33	n.e.	n.e.				
34	n.e.	n.e.				
35	0	1	0	1		biopsy
36	n.e.	n.e.				surgical specimen
37	n.e.	n.e.				surgical specimen
38	n.e.	n.e.				
39	n.e.	n.e.				surgical specimen
40	0	15				surgical specimen
41	5	60				surgical specimen
42	2	35				surgical specimen
43	2	20				biopsy

IC, immune cell score; i.e.; intraepithelial; if, invasion front; tc, tumor center; n.e., not eligible;
TPS, tumor proportional score

Supplementary Table S6. Validation of resistance variants detected by NGS with ddPCR.*

Patient	12				21		30	
Mutation	B2M L15fs				PD-L1 K162fs		PD-L1 L88S	
Timepoint/Material	BL tumor		On-treatment tumor		Liquid Biopsy at EOT		Liquid Biopsy at EOT	
detection method	NGS	ddPCR	NGS	ddPCR	NGS	ddPCR	NGS	ddPCR
VAF in [%]	7	7.02	0.89	0.85	3.1	0.06	2.7	5.25

Patient	22															
Mutation	B2M L15fs						PD-L1 L88S						JAK1 H183Y			
Timepoint/Material	BL tumor		On-treatment bladder sample		On-treatment rectum sample		BL tumor		On-treatment bladder sample		On-treatment rectum sample		BL tumor		On-treatment bladder sample	
detection method	NGS	ddPCR	NGS	ddPCR	NGS	ddPCR	NGS	ddPCR	NGS	ddPCR	NGS	ddPCR	NGS	ddPCR	NGS	ddPCR
VAF in [%]	0	0.38	31	34.1	31	37.2	0	0.09	43	29.1	11.8	27.7	0	0.19	11	14.9

* The specificity of each mutant probe was validated on gBlocks with wild-type or mutant sequence.

Supplementary Table S7. Genetic information and variant allele frequencies on FCGR2A and FCGR3A SNPs.

Pat ID	Gene	Chrom	pos	HGVS.p	HGVS.c	ID	REF	ALT	DP	UMT	VMF
1	FCGR2A	chr1	161479745	p.His167Arg	c.500A>G	rs1801274	A	G	94026	594	1.00
2	FCGR2A	chr1	161479745	p.His167Arg	c.500A>G	rs1801274	A	G	62765	362	0.49
3	FCGR2A	chr1	161479745	p.His167Arg	c.500A>G	rs1801274	A	G	24876	872	1.00
4	FCGR2A	chr1	161479745	p.His167Arg	c.500A>G	rs1801274	A	G	18015	1583	0.50
5	FCGR2A	chr1	161479745	p.His167Arg	c.500A>G	rs1801274	A	G	12236	857	0.56
6	FCGR2A	chr1	161479745	p.His167Arg	c.500A>G	rs1801274	A	G	79943	1662	0.48
8	FCGR2A	chr1	161479745	p.His167Arg	c.500A>G	rs1801274	A	G	8012	1738	0.50
12	FCGR2A	chr1	161479745	p.His167Arg	c.500A>G	rs1801274	A	G	45626	2737	0.55
15	FCGR2A	chr1	161479745	p.His167Arg	c.500A>G	rs1801274	A	G	16268	560	0.48
16	FCGR2A	chr1	161479745	p.His167Arg	c.500A>G	rs1801274	A	G	17675	227	0.42
17	FCGR2A	chr1	161479745	p.His167Arg	c.500A>G	rs1801274	A	G	21035	1516	0.50
18	FCGR2A	chr1	161479745	p.His167Arg	c.500A>G	rs1801274	A	G	30057	1488	1.00
20	FCGR2A	chr1	161479745	p.His167Arg	c.500A>G	rs1801274	A	G	25249	652	0.50
21	FCGR2A	chr1	161479745	p.His167Arg	c.500A>G	rs1801274	A	G	62650	1400	0.47
22	FCGR2A	chr1	161479745	p.His167Arg	c.500A>G	rs1801274	A	G	27465	1929	0.61
23	FCGR2A	chr1	161479745	p.His167Arg	c.500A>G	rs1801274	A	G	19039	352	0.49
24	FCGR2A	chr1	161479745	p.His167Arg	c.500A>G	rs1801274	A	G	106828	701	0.59
25	FCGR2A	chr1	161479745	p.His167Arg	c.500A>G	rs1801274	A	G	26199	1384	0.52
26	FCGR2A	chr1	161479745	p.His167Arg	c.500A>G	rs1801274	A	G	25859	1993	0.49
27	FCGR2A	chr1	161479745	p.His167Arg	c.500A>G	rs1801274	A	G	94129	900	0.50
29	FCGR2A	chr1	161479745	p.His167Arg	c.500A>G	rs1801274	A	G	39474	2014	0.49
31	FCGR2A	chr1	161479745	p.His167Arg	c.500A>G	rs1801274	A	G	33376	1611	0.48
32	FCGR2A	chr1	161479745	p.His167Arg	c.500A>G	rs1801274	A	G	20842	172	0.51
33	FCGR2A	chr1	161479745	p.His167Arg	c.500A>G	rs1801274	A	G	24262	324	1.00
34	FCGR2A	chr1	161479745	p.His167Arg	c.500A>G	rs1801274	A	G	25388	282	1.00
35	FCGR2A	chr1	161479745	p.His167Arg	c.500A>G	rs1801274	A	G	22444	288	0.99
36	FCGR2A	chr1	161479745	p.His167Arg	c.500A>G	rs1801274	A	G	64916	302	0.48
37	FCGR2A	chr1	161479745	p.His167Arg	c.500A>G	rs1801274	A	G	1336	146	0.58
38	FCGR2A	chr1	161479745	p.His167Arg	c.500A>G	rs1801274	A	G	92058	1331	0.53
39	FCGR2A	chr1	161479745	p.His167Arg	c.500A>G	rs1801274	A	G	20842	172	0.51
40	FCGR2A	chr1	161479745	p.His167Arg	c.500A>G	rs1801274	A	G	39480	2929	0.51
41	FCGR2A	chr1	161479745	p.His167Arg	c.500A>G	rs1801274	A	G	24937	2279	0.50
42	FCGR2A	chr1	161479745	p.His167Arg	c.500A>G	rs1801274	A	G	23600	1787	0.50
43	FCGR2A	chr1	161479745	p.His167Arg	c.500A>G	rs1801274	A	G	2172	61	0.46
5	FCGR3A	chr1	161514542	p.Phe212Val	c.634T>G	rs396991	A	C	15587	761	0.42
7	FCGR3A	chr1	161514542	p.Phe212Val	c.634T>G	rs396991	A	C	8385	887	0.45
8	FCGR3A	chr1	161514542	p.Phe212Val	c.634T>G	rs396991	A	C	6253	577	0.43
11	FCGR3A	chr1	161514542	p.Phe212Val	c.634T>G	rs396991	A	C	3409	15	0.55
13	FCGR3A	chr1	161514542	p.Phe212Val	c.634T>G	rs396991	A	C	23904	962	0.43
19	FCGR3A	chr1	161514542	p.Phe212Val	c.634T>G	rs396991	A	C	3948	82	0.52
21	FCGR3A	chr1	161514542	p.Phe212Val	c.634T>G	rs396991	A	C	22966	213	1.00
22	FCGR3A	chr1	161514542	p.Phe212Val	c.634T>G	rs396991	A	C	17670	264	1.00
24	FCGR3A	chr1	161514542	p.Phe212Val	c.634T>G	rs396991	A	C	11871	143	0.41
29	FCGR3A	chr1	161514542	p.Phe212Val	c.634T>G	rs396991	A	C	13284	552	0.45

30	FCGR3A	chr1	161514542	p.Phe212Val	c.634T>G	rs396991	A	C	29396	818	0.43
31	FCGR3A	chr1	161514542	p.Phe212Val	c.634T>G	rs396991	A	C	31359	975	0.46
40	FCGR3A	chr1	161514542	p.Phe212Val	c.634T>G	rs396991	A	C	19519	456	0.19